Available online at www.sciencedirect.com

SciVerse ScienceDirect

Ceramics International 39 (2013) 3569–3575

CERAMICS INTERNATIONAL

www.elsevier.com/locate/ceramint

Graphene modified Nd/TiO_2 photocatalyst for methyl orange degradation under visible light irradiation

N.R. Khalid[a,b,*], E. Ahmed[b], Zhanglian Hong[a,**], Yuewei Zhang[a], Mahtab Ullah[b], M. Ahmed[a,b]

[a]*State Key Laboratory of Silicon Materials and Department of Materials Science and Engineering, Zhejiang University, Hangzhou 310027, PR China*
[b]*Department of Physics, Bahauddin Zakariya University, Multan 60800, Pakistan*

Received 30 August 2012; received in revised form 9 September 2012; accepted 10 October 2012
Available online 17 October 2012

Abstract

A novel nanoscale GR–Nd/TiO_2 composite photocatalyst was synthesized by the hydrothermal method. Its crystal structure, surface morphology, chemical composition and optical properties were studied using XRD, TEM, and XPS, DRS and PL spectroscopy. It was found that graphene and neodymium modification shifts the absorption edge of TiO_2 to visible-light region. The results of photoluminescence (PL) emission spectra show that GR–Nd/TiO_2 composites possess better charge separation capability than do Nd/TiO_2 and pure TiO_2. The photocatalytic activity of prepared samples was investigated by degradation of methyl orange (MO) dye under visible light irradiation. The results show that the GR–Nd/TiO_2 composite can effectively photodegrade MO, showing an impressive photocatalytic activity enhancement over that of pure TiO_2. The enhanced photocatalytic activity of the composite catalyst might be attributed to the large adsorptivity of dyes, extended light absorption range and efficient charge separation due to Nd doping and graphene incorporation.

Keywords: A. Sol–gel processes; B. Nanocomposites; C. Optical properties; D. TiO_2

1. Introduction

Titanium dioxide (TiO_2) has long been targeted for various applications, particularly in environmental pollution control, conversion and energy storage, sensors, photovoltaics and Li batteries because of its unique photo-electric properties [1–4]. TiO_2 has the advantage of good chemical stability, nontoxicity and relatively low cost. However, many problems remain unresolved in the TiO_2 photocatalyst system for practical applications, such as narrow spectrum response range and low separation probability of the photoinduced electron–hole pairs. Therefore, many techniques have been examined to extend the spectral response of TiO_2 into the visible region and to enhance its photocatalytic activity. Doping with metallic cations or non-metallic anions has been widely used for the modification of TiO_2 to improve its photocatalytic activity or to extend its light absorption into visible region [5–14]. It is known that metal ion doping can modify the surface properties of TiO_2, hinder the recombination of photo-generated electron–hole pairs and increase the amount of the active sites. Especially, photocatalytic activity of TiO_2 can be significantly enhanced by doping with the lanthanide ions having 4f configuration. Among them, neodymium doping has attracted more interest due to comparatively large (Nd^{+3}) ion which produces a localized charge perturbation during substitutional doping into TiO_2 lattice and increases its photocatalytic activity [7,10].

Another common method for enhancing the photocatalytic efficiency of TiO_2 is immobilization TiO_2 nanoparticles on a co-adsorbent surface such as mesoporous materials, zeolites, alumina, silica or carbon based materials [15–18]. Among these, carbonaceous materials including activated carbon, carbon nanotubes, and graphene are of great

*Corresponding author at: Department of Physics, Bahauddin Zakariya University, Multan 60800, Pakistan. Tel.: +92 61 9210091; fax: +92 61 9210098.
**Corresponding author. Tel./fax: +86 571 87951234.
E-mail addresses: khalidbzu@gmail.com (N.R. Khalid), hong_zhanglian@zju.edu.cn (Z. Hong).

0272-8842/$ - see front matter © 2012 Elsevier Ltd and Techna Group S.r.l. All rights reserved.
http://dx.doi.org/10.1016/j.ceramint.2012.10.183

interest due to their unique pore structure, electronic properties and adsorption capacity [19–23]. Recently, graphene with its unique structure of one-atom thick planar sheets of sp^2-bonded carbon atoms closely packed in a honeycomb crystal lattice has attracted a great deal of scientific interest due to its excellent mechanical, electrical, thermal, optical and surface properties [23]. As compared with other carbonaceous materials, graphene has many advantages, including high surface area, high transparency and good interfacial contact with adsorbents. Therefore, it is advantageous to investigate simple and effective approaches for preparing graphene based composites and expand their practical applications. Due to conjugated structure of graphene, the combination of TiO_2 and graphene may be an ideal preference to achieve an enhanced charge separation in electron-transfer processes. In a recent investigation, P25–TiO_2 dispersed on graphene nanosheet was reported to show enhanced photocatalytic activity [24]. Williams et al. mixed ultrasonically TiO_2 particles and graphene oxide (GO) colloids, followed by UV-assisted photocatalytic reduction of GO to prepare TiO_2–graphene composites [25]. In another case, TiO_2–graphene composite materials were prepared by self-assembly of TiO_2 nanoparticles grown on graphene by a one-step approach with the assistance of an anionic surfactant [21]. Zhang et al. [22] prepared P25–graphene composite for methyl blue degradation using a hydrothermal method. Sonophototcatalytic activity of graphene oxide based Pt–TiO_2 composites for DBS degradation was investigated by Neppolian et al. [26]. Farhangi et al. [27] prepared Fe doped TiO_2 nanowires on graphene sheets for photodegradation of 17β-estradiol (E_2). Nevertheless, understanding of metal doped TiO_2/graphene photocatalysis system is unclear.

In this study, we have synthesized Nd doped TiO_2 (Nd/TiO_2) nanoparticles by the sol–gel method and then successfully decorated on graphene sheets by hydrothermal process. The effect of neodymium doping on TiO_2 and graphene–TiO_2 (GR–TiO_2) composite catalysts was investigated by degradation of methyl orange dye under visible-light illumination as a model reaction. The prepared GR–Nd/TiO_2 composites showed extended visible-light absorption and enhanced photocatalytic activity than those of pure TiO_2.

2. Experimental

2.1. Preparation of Nd doped TiO_2

The neodymium doped TiO_2 samples were synthesized by the sol–gel method [28]. Firstly, required amounts of tetrabutyl titanate and 10 ml acetic acid were added to 50 ml absolute ethanol (solution A). Secondly, given amounts of $Nd(NO_3)_3 \cdot 6H_2O$, 5 ml acetic acid and 6.25 ml distilled water were added to 25 ml ethanol (solution B). Then solution B was added dropwise into solution A with vigorous magnetic stirring. The obtained mixture was stirred for 3 h, and then kept at room temperature in air for 24 h to form aged homogeneous gel. The as prepared gel was dried at 80 °C in an oven and then the gel was porphyrized into powder and calcined at 450 °C in a furnace for 2 h to obtain Nd doped TiO_2 nanopowder. The atomic ratios of Nd to TiO_2 were 0.6%, 1.2% and 2.0% and the samples obtained were labeled as 0.6Nd/TiO_2, 1.2Nd/TiO_2, and 2.0Nd/TiO_2 respectively.

2.2. Preparation of GR–Nd/TiO_2 composites

Graphene oxide (GO) was synthesized from graphite powder (99.99% Alfa Aesar) by a modified Hummers method [29]. More details on these aspects are given in our previous study [30]. GR–Nd/TiO_2 composites were obtained via a hydrothermal method based on Zhang's work with little modifications [22]. Briefly, 20 mg of graphene oxide was dissolved in a solution of distilled water (80 ml) and ethanol (40 ml) by ultrasonic treatment for 3 h, and then 200 mg of TiO_2 or Nd/TiO_2 was added and stirred for another 2 h to get a homogeneous suspension. The suspension was then placed in a 200 ml Teflon-sealed autoclave and maintained at 120 °C for 3 h to simultaneously achieve the reduction of graphene oxide and the deposition of TiO_2 on the graphene sheets. Finally, the resulting composite was recovered by filtration, rinsed by deionized water 10 times, and dried at 70 °C for 12 h.

2.3. Characterization

Powder X-ray diffraction (XRD) patterns were collected from 10° to 80° in 2θ with 0.02° step/s using a Rigaku D/max-3B X-ray diffractometer with Cu Kα as the radiation source ($\lambda = 0.15406$ nm) at 40 kV and 36 mA. Transmission electron spectroscopy (TEM) study was carried out on a JEOL JEM-1200EX electron microscope instrument operated at 200 kV. The samples for TEM were prepared by dispersing the final powder in ethanol and the dispersion was then dropped on carbon–copper grids. Chemical compositions of composites were analyzed using X-ray photoelectron spectroscopy (Thermo-VG Scientific, ESCALAB250, monochromatic Al K_α X-ray source). All binding energies were referenced to the C 1s peak (284.6 eV) arising from adventitious carbon. UV–vis diffuse reflectance spectra (DRS) were measured in the range of 300–800 nm using a HITACHI U-4100 UV–vis spectrometer with an integrating sphere accessory. The powders were pressed into pellets, and $BaSO_4$ was used as a reference standard for the correction of instrumental background. Their reflectance was converted to absorbance by the Kubelka–Munk function: $F(R) \propto K/S = (1-R)^2/2R$, where K is the molar absorption coefficient, S is the scattering coefficient, and R is the diffuse reflectance. The photoluminescence (PL) emission spectra were carried out at room temperature with a F-4500 fluorescence spectrophotometer (Hitachi) using a Xe lamp as radiation source.

2.4. Measurement of photocatalytic activity

The photocatalytic activities of different samples were estimated by monitoring the degradation of methyl orange (MO) in a self-assembled apparatus with a metal halogen lamp (HQIBT, 400W/D, OSRAM, Germany) as the radiation source. The visible-light ($\lambda \geq 420$ nm) used during the experiment was obtained by a filter with cut-off wavelength of 420 nm. Typically, for the photocatalytic experiment, 100 mg photocatalyst was suspended in 100 ml MO aqueous solution with a concentration of 10 mg l^{-1} in a beaker. The suspension was magnetically stirred for 30 min to reach the adsorption/desorption equilibrium without visible light exposure. Following this, the photocatalytic reaction was started by the exposure of visible light. The temperature of the suspension was kept at about 20 °C by an external cooling jacket with recycled water. After a setup exposure time, 5 ml suspension was sampled, centrifuged, and the supernatant was taken out for UV–vis absorption measurement. The intensity of the main absorption peak (464 nm) of the MO dye was referred to as a measure of the residual dye concentration (C).

3. Results and discussion

XRD patterns of Nd doped TiO_2 and GR–Nd/TiO_2 composites with different Nd dopings are shown in Fig. 1. The patterns clearly show peaks of anatase phase structure of TiO_2, namely, the planes (101), (004), (200), (211), (204), (220), and (215) at 2θ values of ca. 25.38, 37.82, 48.18, 55.2, 62.92, 69.92, and 74.9 respectively, all of which are in good agreement with JCPDS-21-1272. In all Nd doped samples, no separate phase of Nd_2O_3 was detected, indicating that Nd^{3+} can enter the lattice of TiO_2 or Nd_2O_3 disperses homogeneously on the surface of TiO_2 [8].

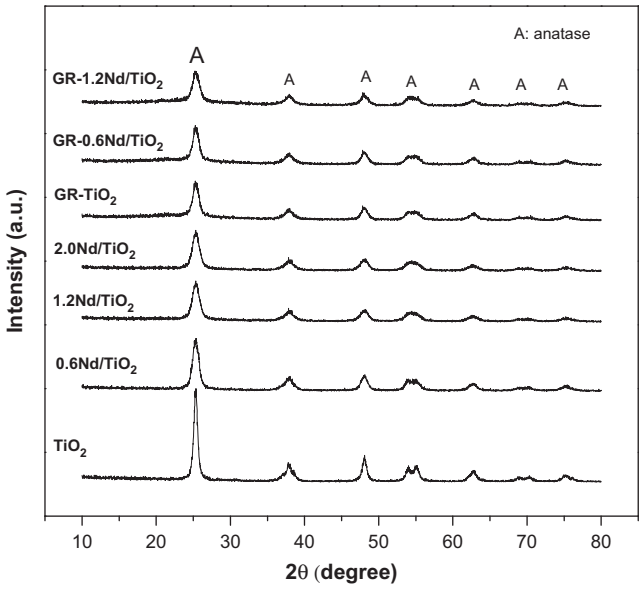

Fig. 1. XRD patterns of Nd/TiO_2, GR–Nd/TiO_2 composites with various Nd contents.

The crystallite sizes (d) of the samples were calculated from full-width at half-maxima of the (101) peak of the anatase TiO_2 by the Debye–Sherrer equation:

$$d = k\lambda/\beta\cos\theta$$

where k is the shape factor of the particle (it is 1 if the spherical shape is assumed) d represents the crystallite size, λ represents the wavelength of incident X-ray, β is full width at half maximum (FWHM) of diffraction peak and θ represents the scattering angle. The average crystallite size calculated from above equation were found to be 13 nm for pure TiO_2 and 11.2 nm, 9 nm, 7 nm for 0.6Nd/TiO_2, 1.2Nd/TiO_2, 2.0Nd/TiO_2 samples respectively. It implies that the Nd doping might restrain the growth of TiO_2 crystallites [10]. Furthermore, characteristic peaks of graphene were not seen in the composite samples, which may be attributed to the fact that addition of graphene would not change the crystalline structure of TiO_2.

Particle size and morphology of the catalysts were recorded using TEM and are shown in Fig. 2a and b. Images from pure TiO_2 and Nd doped TiO_2 powder samples exhibited highly uniform nanocrystalline structures with observed particle size in (8–12) nm range and are in good agreement with XRD results. Fig. 2c and d shows the image results of GR–TiO_2 and GR–1.2Nd/TiO_2 composites, which display that the base of TiO_2 and Nd/TiO_2 nanoparticles is graphene.

Fig. 3 shows the XPS survey spectra of GR–1.2Nd/TiO_2 composite, which contains 0.65% Nd 4d, 49% O 1s, 26% Ti 2p and 24.35% C 1s. In core level XPS spectrum of Ti 2p (Fig. 4), the Ti 2p3/2 and Ti 2p1/2 peaks are located at binding energies of 459.4 eV and 465.2 eV respectively, which is consistent with the value of Ti^{4+} in the TiO_2 lattice [31]. O 1s core level spectrum shows the main peak at 530.3 eV due to the metallic oxides Ti–O bond, which is consistent with binding energy of O^{2-} in the TiO_2 lattice [31]. The peak at 530.9 eV is for oxygen atoms in the surface hydroxyl groups (H–O bonds) and/or in the carboxyl groups (C–O bonds) and the peak appearing at 532.7 eV can be attributed to adsorbed OH^- on the surface of TiO_2 [32]. In high-resolution XPS spectrum of C1s, the main peak was observed at 284.6 eV, which corresponds to the adventitious carbon adsorbed on the surface of sample, the second peak at 285.6 is ascribed to elemental carbon and the peak at 288.8 eV corresponds to C═O bonds implying coordination bonding between Ti and carboxylic acids on the surface of graphene sheets [27,32]. Finally, Nd 4d peak at about 122 eV, which shows positive shift from a metallic Nd^0 peak position (118 eV) results from the decrease of electron density, suggesting that the dopant may be present as a Nd^{3+} ion in the TiO_2 nanopowder [9,10].

UV–vis diffuse reflectance spectra (DRS) of Nd/TiO_2 and GR–Nd/TiO_2 composite photocatalysts with neodymium doping are shown in Fig. 5. The spectra show the absorption edge of pure TiO_2 powder to be about 388 nm as commonly observed for anatase TiO_2, which is attributed to band–band transition. However, all Nd doped TiO_2 samples exhibit extended light absorption in the visible-light region, and yield

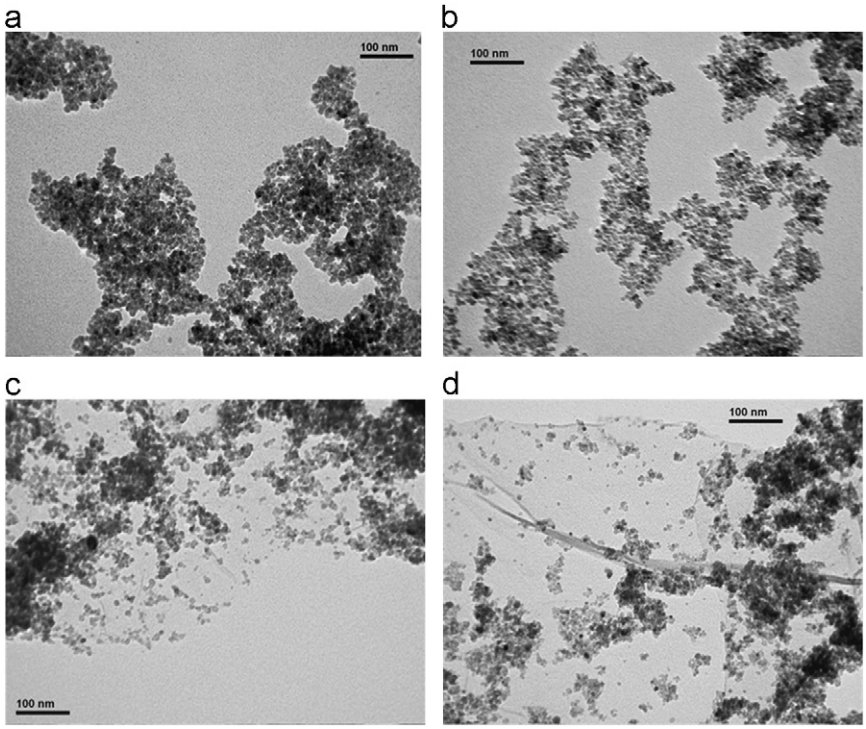

Fig. 2. TEM images of (a) TiO_2, (b) 1.2Nd/TiO_2, (c) GR–TiO_2, and (d) GR–1.2Nd/TiO_2.

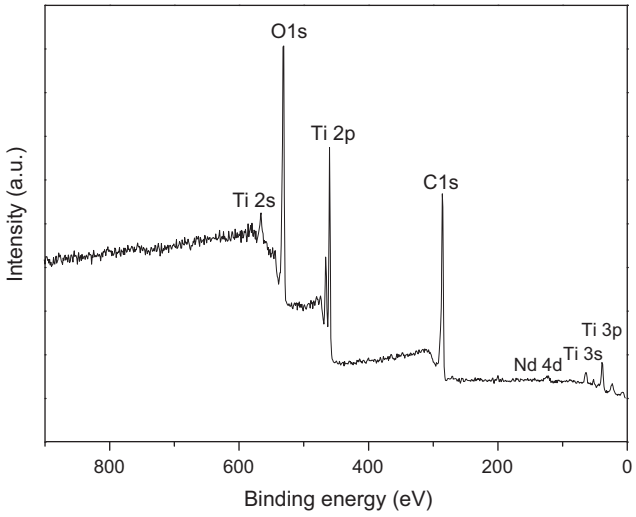

Fig. 3. XPS survey spectra of GR–1.2Nd/TiO_2 composite.

a redshift compared to pure TiO_2. Redshift of this type can be ascribed to the charge transfer transitions between the Nd and TiO_2 conduction or valence band [13,33]. Furthermore, a noticable increase of absorption in visible-light region was also observed after modification of Nd/TiO_2 photocatalyst with graphene, which might be attributed to the fact that incorporation of graphene increased light absorption of TiO_2 in visible range, similar to TiO_2–CNT and C-doped TiO_2 [22].

The study of the photoluminescence emission spectra is a useful method to investigate the efficiency of charge carrier trapping, emigration, transfer and to understand the fate of electron–hole pairs in the field of photocatalysis over solid semiconductors [32,34]. It is known that the PL emission is the result of the recombination of excited electrons and holes either directly (band–band) or indirectly (via a bandgap state). Fig. 6 shows the photoluminscence spectra of TiO_2, Nd/TiO_2 and GR–Nd/TiO_2 composites. The PL intensity of TiO_2 is highest among all the samples, demonstrating the recombination of electrons and holes although the PL intensity decreased in both the Nd doped TiO_2 nanoparticles and the graphene modified Nd/TiO_2 composites compared to pure TiO_2. Among all the samples the lowest intensity was observed for the GR–1.2Nd/TiO_2 composite, showing that the charge carriers were separated more effectively due to cooperative effect of neodymium doping and graphene.

Nd/TiO_2 and GR–Nd/TiO_2 composites were studied by photodegradation of methyl orange as model reaction under visible-light irradiation. MO degradation experiment without catalyst was carried out under the same condition. The resulting photolysis was ignored because the corresponding degradation was only 0.4% after 3 h visible-light irradiation. Fig. 7a presents the results of photocatalytic activity of different samples. It is observed that Nd doping enhanced the photocatalytic activity of the catalysts with increasing doping amount upto 1.2%. However, when doping of Nd exceeds this level, a decrease in photocatalytic activity was observed, so optimal dosage of neodymium ion was found to be 1.2%. This dosage of Nd doping achieved the most efficient separation of electron–hole pairs in our Nd/TiO_2 samples (as confirmed in PL results). Phototcatalytic degradation of methyl orange follows roughly the pseudo-first-order reaction

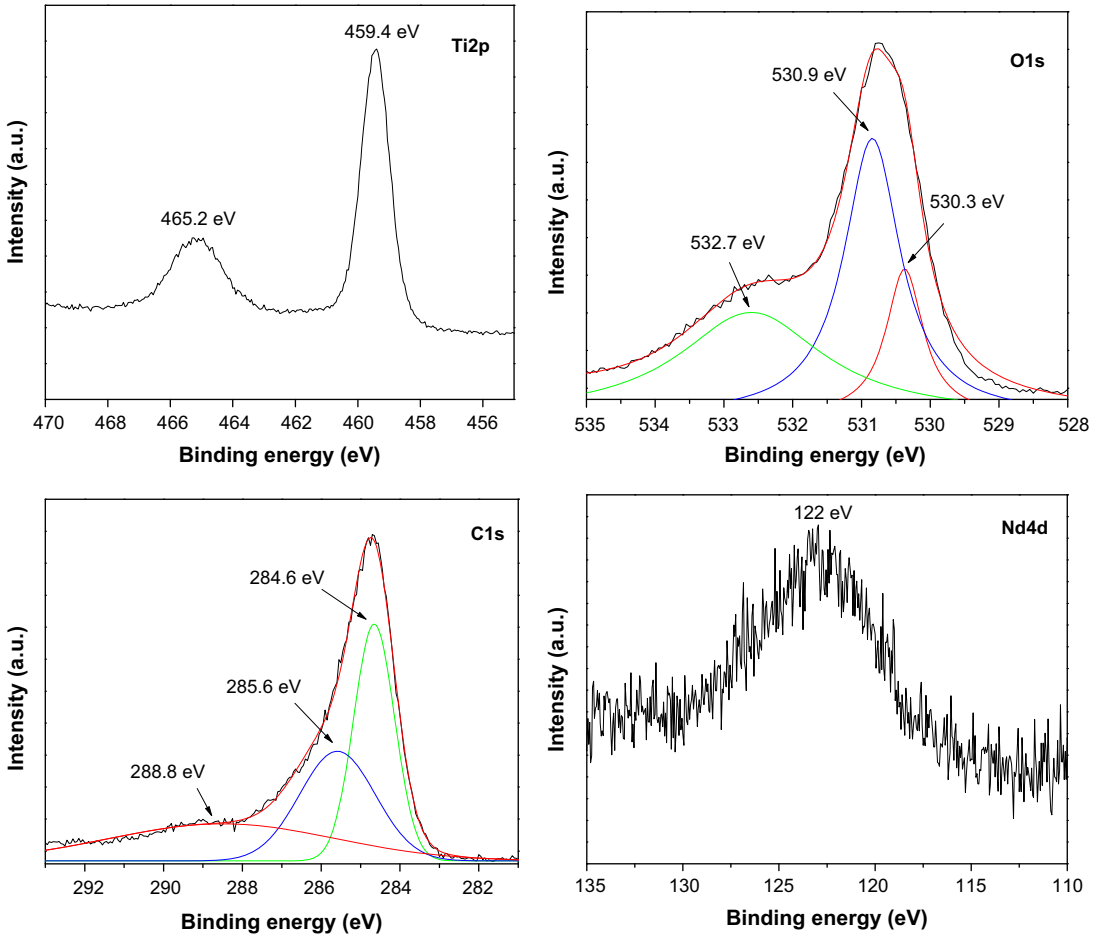

Fig. 4. XPS core level spectra of Ti 2p, O 1s, C 1s and Nd 4d of GR–1.2Nd/TiO_2 composite sample.

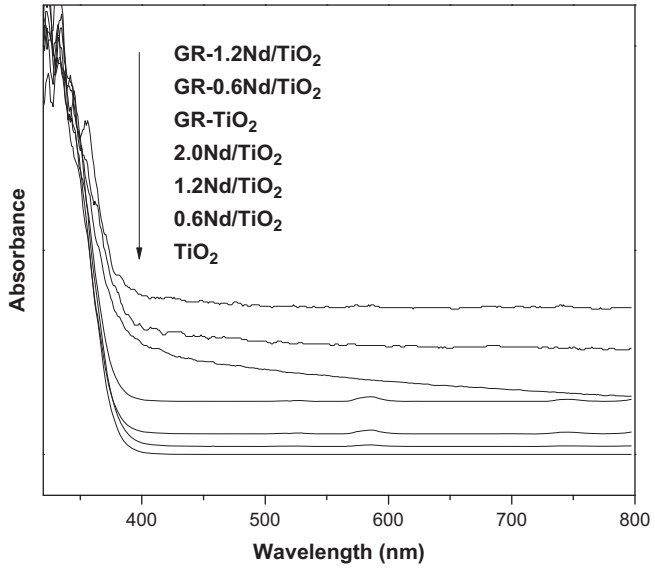

Fig. 5. UV–visible diffuse reflectance spectra of TiO_2 and GR–TiO_2 with various Nd contents.

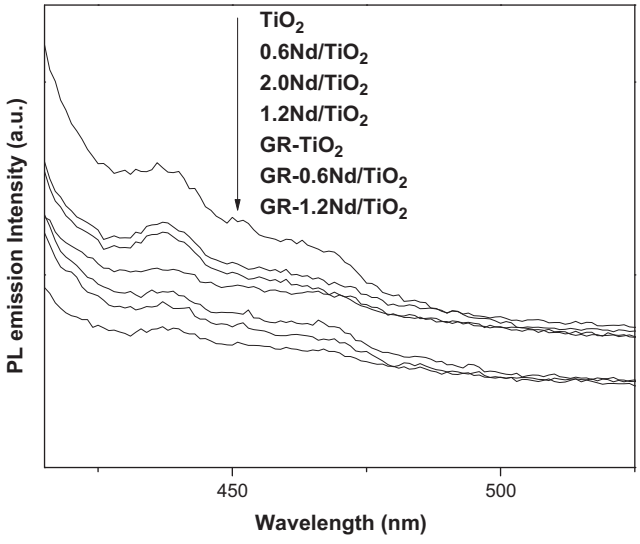

Fig. 6. Photoluminescence emission spectra of TiO_2 and GR–TiO_2 composites with Nd doping (excitation wavelength of 380 nm).

kinetics for low dye concentrations [23]:

$$\ln(C_0/C) = k_{app}t$$

where k_{app} is the apparent first order kinetic constant, used as the basic kinetic parameter for different photocatalysts. C_0 is the initial concentration of MO in aqueous solution

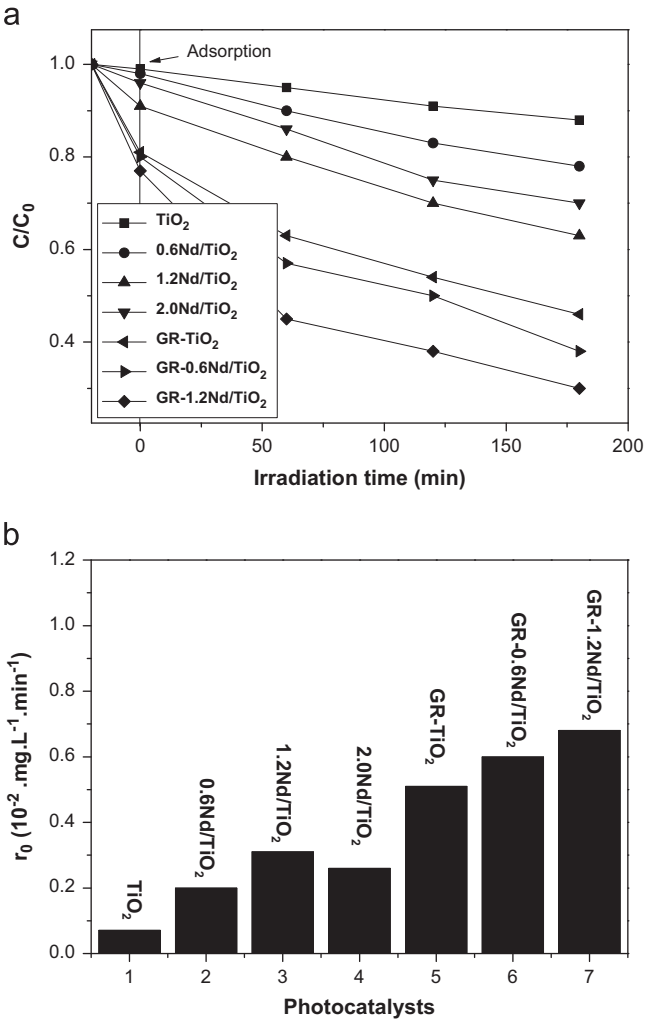

Fig. 7. (a) Effect of the catalysts on the methyl orange photodegradation and (b) the initial degradation rate (r_0) of methyl orange in the presence of different catalysts under visible light irradiation.

and C is the residual concentration of MO at time t. The apparent constant values could be deduced from the linear fitting of $\ln(C_0/C)$ vs irradiation time. The initial degradation rate ($r_0 = k_{app}C_0$) of 10 mg l^{-1} MO with different catalysts was calculated and the results are presented in Fig. 7b.

The results show that degradation rate (r_0) is enhanced by Nd doping and introducing graphene into the composites. The degradation rate of MO is in the order GR–1.2Nd/TiO_2 > GR–0.6Nd/TiO_2 > GR–TiO_2 > 1.2Nd/TiO_2 > 2.0Nd/TiO_2 > 0.6Nd/TiO_2 > TiO_2. The degradation rate constant for GR–1.2Nd/TiO_2 composite catalyst ($r_0 = 0.68 \times 10^{-2}$/min) was found to be higher than that of pure TiO_2 ($r_0 = 0.07 \times 10^{-2}$/min). Firstly, the enhanced photocatalytic activity of GR–Nd/TiO_2 composite catalyst might be attributed to extended light absorption in visible-light region due to Nd doping and graphene incorporation. Seconly, adsorption onto the catalyst surface is one of the key factors for the degradation of organic compounds during photocatalysis. Prior to irradiation (30 min), the adsorption of MO was monitored. It is obseved that about 23% of the MO was adsorbed for GR–1.2Nd/TiO_2 composite catalyst and is found to be higher compared to those of pure TiO_2, Nd/TiO_2 and GR–TiO_2 composite. Therefore, the higher adsorption of MO onto the catalyst surface is another important reason for the enhanced degradation rate of MO during photocatalysis. Thirdly, graphene in the composite acts as an electron acceptor and transporter. Graphene has been reported to be a competative candidate as an acceptor material due to its π-conjugation structure and has unexpectedly excellent conductivity due to its two dimensional planar structure. Therefore, rapid transport of charge carriers could be achieved and an effective charge separation subsequently accomplished. Overall, both the electron accepting and transporting properties of graphene in the composite contributed to the enhancement of photocatalytic activity [22,26,27]. Finally, the presence of Nd in TiO_2–graphene composites favors the transfer of photoformed electrons to Nd and then Nd acts as a reservoir for photogenerated electrons, thereby promoting an interfacial charge-transfer process. The photoformed electrons can readily be transported through graphene in addition to Nd and hence the rate of degradation of MO is significantly enhanced with graphene and neodymium. It can be attributed to suppressed recombination of electon–hole pairs due to presence of graphene and Nd in the composite photocatalyst. Therefore, it is concluded that cooperative effects of adsorption of MO onto catalyst surface, extended light absorption in visible-light region due to Nd doping and graphene, efficient charge separation and well formed anatase phase played significant role for enhanced photocatalytic activity of composite catalyst under visible-light irradiation.

4. Conclusion

Neodymium doped GR–TiO_2 composite photocatalysts prepared by the hydrothermal method have stronger light absorption in visible-light range and showed enhanced photocatalytic activity than those of TiO_2 under visible-light irradiation for MO degradation. The enhanced photocatalytic activity of the composite catalyst might be attributed to the cooperative effects of extended light absorption, efficient charge separation, enhanced adsorptivity onto the catalyst surface due to giant two-dimensional planar structure of graphene and possibility of more π–π interaction between composite and organic compound. This study open a new possibility in the investigation of graphene–TiO_2 composites and promotes their practical applications in environmental applications.

Acknowledgments

This work was supported partially by the Natural Science Foundation of China (Grant no. 51072180), the China Postdoctoral Science Foundation (Grant no.

20110491764), the Fundamental Research Funds for the Central Universities (Grant no.2009QNA4005), and the State Key Laboratory of Silicon Materials (SKL2009-14) at Zhejiang University. N.R. Khalid thanks to Higher Education Commission of Pakistan for IRSIP scholarship.

References

[1] X. Li, R. Xiong, G. Wei, Preparation and photocatalytic activity of nanoglued Sn-doped TiO_2, Journal of Hazardous Materials 164 (2009) 587–591.
[2] S. Ardizzone, C.L. Bianchi, G. Cappelletti, S. Gialanella, C. Pirola, V. Ragaini, Tailored anatase/brookite nanocrystalline TiO_2. The optimal particle features for liquid and gas-phase photocatalytic reactions, Journal of Physical Chemistry C 111 (2007) 13222–13231.
[3] M. Li, P. Tang, Z. Hong, M. Wang, Colloid—High efficient surface-complex-assisted photodegradation of phenolic compounds in single anatase titania under visible-light, Colloids and Surfaces A: Physicochemical and Engineering Aspects 318 (2008) 285–290.
[4] M. Li, Z. Hong, Y. Fang, F. Huang, Synergistic effect of two surface complexes in enhancing visible-light photocatalytic activity of titanium dioxide, Materials Research Bulletin 43 (2008) 2179–2186.
[5] H. Cuiying, Y. Wansheng, D. Liqin, L. Zhibin, S. Zhengang, Z. Lancui, Effect of Nd^{3+} doping on photocatalytic activity of TiO_2 nanoparticles for water decomposition to hydrogen, Chinese Journal of Catalysis 27 (2006) 203–209.
[6] W. Li, A.I. Frenkel, J.C. Woicik, C. Ni, S.I. Shah, Dopant location identification in Nd^{3+}-doped TiO_2 nanoparticles, Physical Review B 72 (2005) 155315–155316.
[7] S. Rengaraj, S. Venkataraj, J.W. Yeon, Y. Kim, X.Z. Li, G.K.H. Pang, Preparation, characterization and application of Nd–TiO_2 photocatalyst for the reduction of Cr(VI) under UV light illumination, Applied Catalysis B: Environmental 77 (2007) 157–165.
[8] W. Xiaohong, S. Peibo, L. Huiling, Q. Lili, Photocatalytic degradation of rhodamine B under visible light with Nd-doped titanium dioxide films, Journal of Rare Earths 27 (2009) 739–743.
[9] H. Meifang, L. Fangbai, L. Ruifeng, W. Hongfu, Z. Guoyi, X. Kechang, Mechanisms of enhancement of photocatalytic properties and activity of Nd^{+3}-doped TiO_2 for methyl orange degradation, Journal of Rare Earths 22 (2004) 542–546.
[10] V. Stengl, S. Bakardjieva, N. Murafa, Preparation and photocatalytic activity of rare earth doped TiO_2 nanoparticles, Materials Chemistry and Physics 114 (2009) 217–226.
[11] R. Asahi, T. Morikawa, T. Ohwaki, K. Aoki, Y. Taga, Visible-light photocatalysis in nitrogen-doped titanium oxides, Journal of Science 293 (2001) 269–271.
[12] J.M. Herrmann, Heterogeneous photocatalysis: fundamentals and applications to the removal of various types of aqueous pollutants, Catalysis Today 53 (1999) 115–129.
[13] J. Wang, D.N. Tafen, J.P. Lewis, Z. Hong, A. Manivannan, M. Zhi, M. Li, N.Q. Wu, Origin of the photocatalytic activity of nitrogen-doped TiO_2 nanobelts, Journal of the American Chemical Society 131 (2009) 12290–12297.
[14] D. Tafen, J. Wang, N.Q. Wu, J.P. Lewis, Visible light photocatalytic activity in nitrogen-doped TiO_2 nanobelts, Applied Physics Letters 94 (2009) 093101.
[15] S. Fukahori, H. Ichiura, T. Kitaoka, H. Tnaka, Photocatalytic decomposition of bisphenol A in water using composite TiO_2-zeolites sheets prepared by a papermaking technique, Environmental Science and Technology 37 (2003) 1048–1051.
[16] A.M. Turek, I.E. Wachs, E. De Canio, Acidic properties of alumina-supported catalysts: and infrared spectroscopy study, The Journal of Physical Chemistry 96 (1992) 5000–5007.
[17] J. Aguado, R. Van Grieken, M.J. Lopez-Munos, J. Marugan, A comprehensive study of the synthesis, characterization and activity of TiO_2 and TiO_2/SiO_2 mixed photocatalysts, Journal of Applied Catalysis: A 312 (2006) 202–212.
[18] J. Matos, A. Garcia, P.S. Poon, Environmental green chemistry applications of nanoporous, Carbons, Journal of Materials Science 18 (2010) 4934–4944.
[19] J. Matos, A. Garcia, T. Cordero, J.M. Chovelon, C. Ferronato, Eco-friendly TiO_2–AC photocatalyst for the selective photooxidation of 4-chlorophenol, Catalysis Letters 130 (2009) 568–574.
[20] K. Woan, G. Pyrigiotakis, W. Sigmund, Photocatalytic carbon-nanotube–TiO_2 composites, Advanced Materials 21 (2009) 2233–2239.
[21] D. Wang, D. Choi, J. Li, Z. Yang, Z. Nie, R. kou, D. Hu, C. Wang, L.V. Saraf, J. Zhang, Assembled TiO_2–graphene hybrid nanostructures for enhanced Li-ion insertion, ACS Nano 3 (2009) 907–914.
[22] H. Zhang, X. Lv, Y. Li, Y. Wang, J. Li, P25–Graphene composite as a high performance photocatalyst, ACS Nano 4 (2009) 380–386.
[23] S. Wang, S. Zhou, Photodegradation of methyl orange by photocatalyst of CNTs/P–TiO_2 under UV and visible-light irradiation, Journal of Hazardous Materials 185 (2011) 77–85.
[24] X.Y. Zhang, H.P. Li, X.L. Cui, Y. Lin, Graphene/TiO_2 nanocomposites: synthesis, characterization and application in hydrogen evolution from water photocatalytic splitting, Journal of Materials Chemistry 20 (2010) 2801–2806.
[25] G. Williams, B. Seger, P.V. Kamat, TiO_2–graphene nanocomposites. UV-assisted photocatalytic reduction of graphene oxide, ACS Nano 2 (2008) 1487–1491.
[26] B. Neppolian, A. Bruno, C.L. Bianchi, M. Ashokkumar, Graphene oxide based Pt–TiO_2 photocatalyst: ultrasound assisted synthesis, characterization and catalytic efficiency, Ultrasonics Sonochemistry 19 (2012) 9–15.
[27] N. Farhangi, R.R. Chowdhury, Y. Medina-Gonzalez, M.B. Ray, P.A. Charpentier, Visible light active Fe doped TiO_2 nanowires grown on graphene using supercritical CO_2, Applied Catalysis B: Environmental (2011).
[28] Y. Su, Y. Xiao, Y. Li, Y. Du, Y. Zhang, Preparation, photocatalytic performance and electronic structures of visible light driven Fe–N co-doped TiO_2 nanoparticles, Materials Chemistry and Physics 126 (2011) 761–768.
[29] W.S. Hummers, R.E. Offeman, Preparation of graphitic oxide, Journal of the American Chemical Society 80 (1958) 1339.
[30] N.R. Khalid, Z. Hong, E. Ahmed, Y. Zhang, H. Chan, M. Ahmad, Synergistic effects of Fe and graphene on photocatalytic activity enhancement of TiO_2 under visible light, Applied Surface Science 258 (2012) 5827–5834.
[31] B. Erdem, R.A. Hunsicker, G.W. Simmons, E.D. Sudol, V.L. Dimonie, M.S. El-Aasser, XPS and FTIR surface characterization of TiO_2 particles used in polymer encapsulation, Langmuir 17 (2001) 2664–2669.
[32] Y. Wu, J. Zhang, L. Xiao, F. Chen, Properties of carbon and iron modified TiO_2 photocatalyst synthesized at low temperature and photodegradation of acid orange 7 under visible light, Applied Surface Science 256 (2010) 4260–4268.
[33] J. Liu, H. Bai, Y. Wang, Z. Liu, X. Zhang, D.D. Sun, Self-assembling TiO_2 nanorods on large graphene oxide sheets at a two-phase interface and their anti-recombination in photocatalytic applications, Advanced Functional Materials 20 (2010) 4175–4181.
[34] K. Akihiko, N. Ryo, I. Akihide, K. Hideki, Effects of doping of metal cations on morphology, activity, and visible light response of photocatalysts, Chemical Physics 339 (2007) 104–110.